# Experimental and numerical study of mean zonal flows generated by librations of a rotating spherical cavity

## A. SAURET[1]†, D. CÉBRON[1], C. MORIZE[1,2] AND M. LE BARS[1]

[1]Institut de Recherche sur les Phénomènes Hors Équilibre, CNRS/Universités Aix-Marseille,
49, rue F. Joliot-Curie, BP 146, F-13384 Marseille cedex 13, France

[2]Laboratoire FAST, UMR 7608, Bat. 502, Campus Universitaire, 91405 Orsay Cedex, France

We study both experimentally and numerically the steady zonal flow generated by longitudinal librations of a spherical rotating container. This study follows the recent weakly nonlinear analysis of Busse (*J. Fluid Mech.*, vol. 650, 2010, pp. 505–512), developed in the limit of small libration frequency–rotation rate ratio and large libration frequency–spin-up time product. Using particle image velocimetry measurements as well as results from axisymmetric numerical simulations, we confirm quantitatively the main features of Busse's analytical solution: the zonal flow takes the form of a retrograde solid-body rotation in the fluid interior, which does not depend on the libration frequency nor on the Ekman number, and which varies as the square of the amplitude of excitation. We also report the presence of an unpredicted prograde flow at the equator near the outer wall.

**Key words:** rotating flows

## 1. Introduction

Longitudinal librations (referred to hereafter as librations) are periodic oscillations of a rotating container about its axis of rotation. Despite the fact that these oscillations are time dependent, it has been recently suggested that they can generate nonlinearly a steady axisymmetric flow in the liquid interior through the Ekman boundary layer (Busse 2010). A better knowledge of this resulting flow is of great interest in geophysics and astrophysics (see for instance Noir *et al.* 2009) where libration is driven by gravitational interactions and is used to investigate the interior structure of planets (e.g. Margot *et al.* 2007; Van Hoolst *et al.* 2008).

In spite of the possible applications, flows driven by libration in rotating containers have not been much studied. Aldridge & Toomre (1969) have observed experimentally that inertial modes can be excited by libration at particular resonance frequencies, which has been confirmed numerically by Rieutord (1991). However, in the case of Aldridge & Toomre (1969), the experimental results are measurements of pressure differences between two points on the axis of rotation, and do not provide information about the resulting flow created in the interior. Tilgner (1999) has investigated numerically the linear response to the forcing in the case of a spherical shell and

has shown that the presence of an inner core only marginally modifies the resonance frequencies. More recently, Noir *et al.* (2009) have studied experimentally by direct flow visualization the presence of centrifugal instabilities in the form of Taylor–Görtler vortices near the outer boundary, by varying the frequency and the amplitude of libration. The same group has also performed laser Doppler velocimetry (LDV) measurements of libration-driven zonal flows in a librating cylinder (Noir *et al.* 2010) in the case of high-frequency librations and axisymmetric simulations in a spherical shell (Calkins *et al.* 2010). Finally, a complete weakly nonlinear theory of the zonal flow driven by low-frequency librations in a sphere has been recently developed by Busse (2010) in the absence of direct resonant forcing of any inertial waves. To our knowledge, the main features of this analytical solution have not been so far validated quantitatively. This is the aim of the present work, combining experimental and numerical approaches. This paper is organized as follows. Section 2 gives a brief summary of the governing equations and the weakly nonlinear analysis of Busse (2010). In §3, we present the experimental set-up and the numerical model used in this study. Then, experimental and numerical results are compared with the theory in §4. Discussion and conclusion are given in §5.

## 2. Weakly nonlinear theory

Let us consider a spherical cavity of radius $R$ filled with a homogeneous and incompressible fluid of kinematic viscosity $\nu$. In the inertial frame, the cavity rotates with an angular velocity

$$\boldsymbol{\Omega}(t) = \left( \Omega_0 + \frac{\Delta\Omega}{2} \cos(\omega_{lib}\, t) \right) \boldsymbol{k}, \tag{2.1}$$

where $\Omega_0$ is the mean rotation rate, $\Delta\Omega$ the amplitude of libration, $\omega_{lib}$ the libration frequency and $\boldsymbol{k}$ is the unit vector in the direction of the rotation axis. Using $R$ and $\Omega_0^{-1}$ as the length scale and time scale, respectively, the dimensionless equations of motion written in the frame rotating at the angular velocity $\Omega_0$ and the sidewall boundary conditions are given by

$$\frac{\partial \boldsymbol{u}}{\partial t} + \boldsymbol{u} \cdot \nabla \boldsymbol{u} + 2\,\boldsymbol{k} \times \boldsymbol{u} = -\nabla p + E\nabla^2 \boldsymbol{u}, \tag{2.2a}$$

$$\nabla \cdot \boldsymbol{u} = 0, \tag{2.2b}$$

$$\boldsymbol{u} = \epsilon\,\boldsymbol{k} \times \boldsymbol{r} \cos(\omega\, t) \quad \text{at } |\boldsymbol{r}| = 1, \tag{2.2c}$$

where $\boldsymbol{r}$ is the spherical radial coordinate, $\boldsymbol{u}$ is the velocity measured in the rotating frame, $p$ is the modified pressure taking into account centrifugal forces, $E = \nu/\Omega_0 R^2$ is the Ekman number, $\epsilon = \Delta\Omega/2\Omega_0$ is the normalized amplitude of libration and $\omega = \omega_{lib}/\Omega_0$ is the normalized librational frequency. The librational forcing appears in the problem through the boundary condition (2.2c). This problem has been recently solved by Busse (2010) in the limit:

$$\sqrt{E} \ll \omega \ll \epsilon \ll 1. \tag{2.3}$$

The limit of small Ekman number allows splitting of the velocity field into two parts: a component $\boldsymbol{U}$ describing the inviscid flow in the interior and a boundary layer component $\boldsymbol{u}$. Following the weakly nonlinear method previously used in the case of precession (Busse 1968) and tidal forcing (Suess 1971), Busse (2010) finds an expression for the steady zonal flow in the inviscid interior $\bar{U}$ in the limit of low
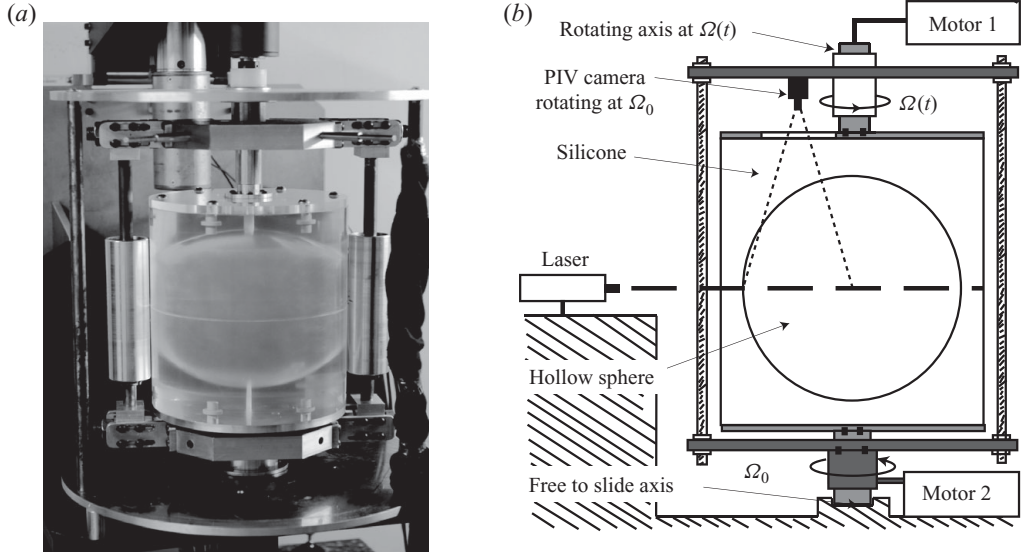
FIGURE 1. (*a*) Photograph and (*b*) sketch of the experimental set-up.

libration frequencies

$$\bar{U} = \epsilon^2 \, \boldsymbol{k} \times \boldsymbol{r} \, f(|\boldsymbol{k} \times \boldsymbol{r}|^2), \tag{2.4a}$$

where

$$f(x^2) = \frac{259 \, x^2 - 360}{2400(1 - x^2)}. \tag{2.4b}$$

The function $f(x^2)$ represents the average difference in angular velocities between the container and the fluid divided by $\epsilon^2$. For $0 \leqslant r \leqslant 1$, $f(x^2)$ is negative, i.e. the fluid is expected to rotate in the retrograde direction. Moreover, this differential rotation is nearly constant up to $r \sim 0.6$ with a mean value of $-0.154$. The zonal flow can thus be assimilated in the bulk to a retrograde solid-body rotation superimposed on the mean rotation, whose amplitude is independent of the libration frequency and the Ekman number and changes as $-0.154 \, \epsilon^2$. In this paper, we verify experimentally and numerically these main features. Note that (2.4*b*) diverges for $x = 1$, i.e. near the outer boundary at the equator. Here, the analytical approach requires the introduction of a specific scaling due to the singularity of the Ekman boundary layer (Busse 2010).

## 3. Methods

### 3.1. *Experimental set-up*

Figure 1 shows a photograph and a schematic view of the experimental set-up used in this study, which is the same as that used by Morize *et al.* (2010) to study zonal flows driven by tides. It consists of a hollow sphere, of radius $R = 10$ cm, which was moulded in a transparent silicone gel to allow flow visualization. The sphere is filled with water and seeded with Optimage particles of 100 μm in diameter and of density 1 g cm$^{-3} \pm 2\%$. The sphere is set in rotation about its vertical axis ($Oz$) with a mean angular velocity $\Omega_0$ up to 85 r.p.m. with a precision of $\pm 0.3\%$. Once a solid-body rotation is reached (typically in $\sim$10 min), a librational motion is set using sinusoidal oscillations of the angular velocity of the sphere of the form $\epsilon \cos(\omega_{lib} \, t)$,

where $\omega_{lib}$ can be chosen between 0.6 and 120 r.p.m. with a precision of $\pm 0.3\,\%$. In terms of dimensionless numbers, we have explored the following ranges: the Ekman number $E = \nu/\Omega_0 R^2 \in [10^{-5}; 10^{-4}]$, the ratio between the libration and the spin frequency $\omega = \omega_{lib}/\Omega_0 \in [0.04; 0.1]$ and the amplitude of libration $\epsilon \in [0.02; 0.15]$ with a precision of $\pm 0.6\,\%$.

In order to measure the velocity field in the equatorial plane induced by librational forcing, we used a rotating particle image velocimetry (PIV) system. A miniature wireless camera, $1/4'$ Sharp HighQ CCD $29.4 \times 22$ mm of resolution $576 \times 768$ pixels, rotates at a constant angular velocity $\Omega_0$ and measurements are made from above through the transparent top surface. The PIV particles are illuminated by a laser sheet of thickness 3 mm produced by a continuous laser (4 W) in the equatorial plane. After turning on the libration forcing, we wait for about 20 oscillations to ensure that the response of the fluid is well established; then we start acquiring pictures of PIV measurements using a video transmitter–receptor system. Velocity fields are computed using DPIVSoft (Meunier & Leweke 2003) on a $60 \times 80$ grid with a spatial resolution of 3 mm, close to the laser sheet thickness. We look for the time-independent axisymmetric zonal flow induced by the libration whereas the forcing of the sphere is of the form $\epsilon\cos(\omega t)$. Velocity fields are thus time-averaged over several periods of libration in order to eliminate the time-dependent term. This also significantly enhances the signal-to-noise ratio. However, our experimental set-up only allows collection of PIV data for a limited time. Hence, we cannot set the libration frequency at too low a value because we would not be able to average out the resulting data over enough periods to have a correct velocity profile. In the experiments, we have considered frequencies in the range $0.04 \leqslant \omega \leqslant 0.1$. Higher and lower libration frequencies have been studied using numerical methods, decribed in the following section.

### 3.2. *Numerical approach*

In addition to the experiments, we have performed axisymmetric numerical simulations of the flow within a sphere of radius $R$ in rotation with an angular velocity $\boldsymbol{\Omega}(t) = \Omega_0(1 + \epsilon\cos(\omega t))\boldsymbol{e}_z$. We use a commercial software, Comsol Multyphisics©, based on the finite elements method to solve this problem. The numerical grid consists of two domains: (i) a boundary layer domain of thickness $0.035\,R$ all along the outer boundary and the axisymmetric axis, which is discretized in the direction normal to the boundary into 25 quadrilateral elements with an initial thickness of $5 \times 10^{-5}\,R$ and a stretching factor of 1.2; (ii) a bulk zone with triangular elements. All elements are of standard Lagrange $P1$–$P2$ type (i.e. linear for the pressure field and quadratic for the velocity field). Note that the finite element method does not induce any particular problem around $r = 0$ and that no stabilization technique has been used in this work. The temporal solver is IDA (Hindmarsh *et al.* 2005), based on backward differencing formulae. At each time step the system is solved with the sparse direct linear solver PARDISO (www.pardiso-project.org). The number of degrees of freedom (DoF) used in the simulations is constant and equal to 157 869 DoF. Our numerical model solves the Navier–Stokes equations in the frame rotating at the velocity $\Omega_0\boldsymbol{e}_z$, with no-slip boundary conditions and a fluid initially at rest in this frame (i.e. a solid-body rotation at $\Omega_0$ in the inertial frame). At time $t = 0$, libration of the outer boundary is turned on and computations are pursued until a stationary state is obtained, which is reached typically in less than 10 libration periods. The velocity is then averaged in time over five libration periods to obtain the steady zonal flow. Results are non-dimensionalized as in the experiment and the theory. The numerical model has been
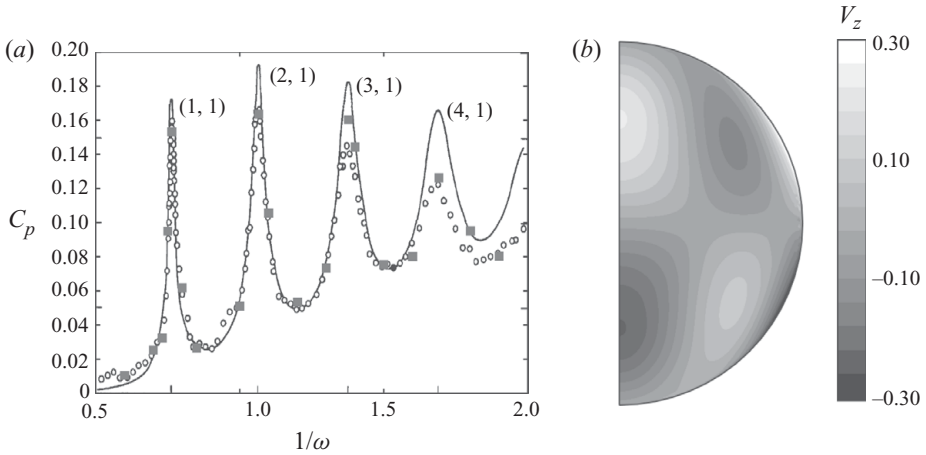
FIGURE 2. (*a*) Time-averaged crest-to-trough amplitude of the pressure difference $C_p$ between the centre and the pole of the sphere for various frequency ratios $\omega = \omega_{lib}/\Omega_0$ and for a libration forcing $\Omega_0 + \tilde{\epsilon}\, \omega_{lib}\, \cos(\omega_{lib}t)$ with $\tilde{\epsilon} = 8.0\,\pi/180$ rad and $Re_\omega = \omega_{lib} R^2/\nu = 6.2 \times 10^4$. The squares represent our numerical values, the circles represent experimental values of Aldridge & Toomre (1969) and the line represents the theoretical plot. (*b*) Velocity in the $z$-direction (i.e. in the direction of the rotation axis) at time $\omega t = 3\pi/2\,[2\pi]$ for the mode $(2,1)$ in the notation of Aldridge & Toomre (1969), corresponding to $1/\omega = 1.066$.

validated in reproducing the experimental results of Aldridge & Toomre (1969). In their paper, they define a fixed libration Reynolds number $Re_\omega = \omega_{lib} R^2/\nu = 6.2 \times 10^4$ and their applied angular velocity is given by

$$\Omega(t) = \Omega_0 + \tilde{\epsilon}\, \omega_{lib}\, \cos(\omega_{lib}t), \qquad (3.1)$$

where $\tilde{\epsilon} = 8.0\,\pi/180$ rad.

Pressure measurements from our numerical simulation when systematically changing the libration frequency $\omega$ are presented in figure 2(*a*) and show an excellent agreement with the experimental results of Aldridge & Toomre (1969) and the numerical results of Rieutord (1991), which validates the numerical model. In figure 2(*a*), each peak corresponds to the resonant forcing of a given inertial mode of the rotating sphere and is labelled by two integers $(n, m)$ (see Aldridge & Toomre 1969). There is no inertial mode for $|\omega| \geqslant 2$ and the modes are progressively damped when $1/\omega$ increases due to the reduced coupling between the container's oscillation and the fluid interior as well as due to the increased viscous damping as the structure of the forced modes becomes more complex. The velocity in the $z$-direction for the mode $(2, 1)$ in the notation of Aldridge & Toomre (1969) is presented in figure 2(*b*) and shows the inertial wave excited by libration forcing as well as the structure of the outer boundary layer. In the next section, following Busse (2010), we investigate the limit $\omega \ll 1$ where the forcing of inertial modes is negligible, but where a global zonal flow is excited.

## 4. Results

Figure 3(*a*) shows an example of the velocity field obtained by PIV measurement in the equatorial plane. The stationary flow is azimuthal and axisymmetric. Besides, as the system rotation is clockwise, the zonal flow corresponds here to a retrograde circulation opposed to the rotation of the sphere. From this velocity field we can
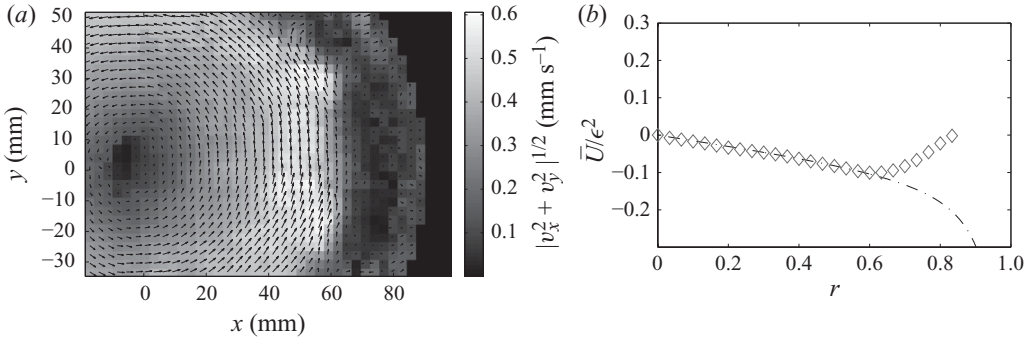
FIGURE 3. (*a*) Time-averaged velocity field obtained by the PIV measurement in the equatorial plane for $E = 1.15 \times 10^{-5}$, $\epsilon = 0.08$ and $\omega = 0.1$. The background is shaded as the norm of the horizontal velocity. The centre of the sphere is at $(0, 0)$. (*b*) Mean experimental dimensionless azimuthal velocity (squares) corresponding to the velocity field of figure 3(*a*) and comparison with the theoretical results of Busse (2010) (dash-dotted line).
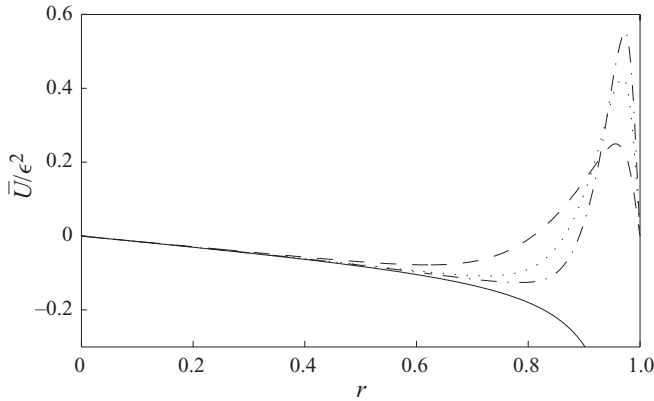


FIGURE 4. Dimensionless time-averaged velocity profiles obtained by numerical simulation in the equatorial plane with $E = 5 \times 10^{-5}$, $\epsilon = 0.2$ and $\omega = 0.03$ (dashed line), $\omega = 0.06$ (dotted line) and $\omega = 0.1$ (dash-dotted line), compared with the inviscid analytical solution of Busse (2010) (solid line).

plot an averaged azimuthal velocity profile at the equator for given parameters in terms of dimensionless quantities as a function of the radial distance (figure 3*b*). Experimentally, because of optical deformation induced by the planar air–silicone and spheroidal silicone–water interfaces, it is not possible to measure the profile for $r > 0.85$. We observe the steady zonal flow visible in figure 3(*a*). Moreover, we can directly compare this dimensionless quantity with the analytical solution given by Busse (2010) and we observe an excellent agreement up to $r \sim 0.6$ with no adjustment parameter. An example of the velocity field obtained numerically is shown in figure 4, which also exhibits good agreement with the analytical solution in the bulk. For $r \geqslant 0.6$, a deviation in the prograde direction with respect to the theoretical profile due to the librating outer boundary is observed and is discussed below. But for now, we concentrate on the mean zonal flow induced in the bulk.

We have performed series of experiments and numerical calculations to systematically check the effect of the three control parameters $E$, $\epsilon$ and $\omega$ on this bulk zonal flow. To do so, we define a reproducible method to synthetize the experimental
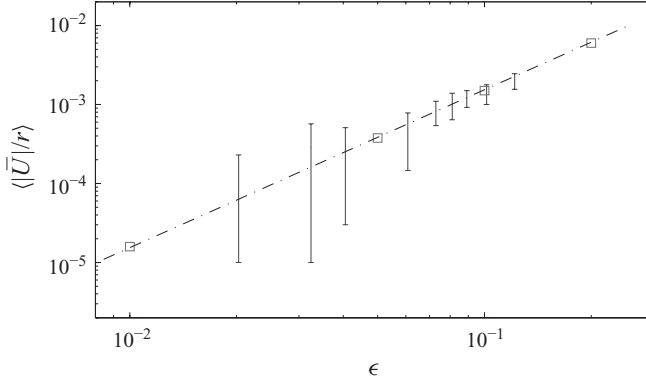
FIGURE 5. Dimensionless average amplitude of $|\bar{U}|/r$ between $r = 0.1$ and $r = 0.6$ as a function of the amplitude $\epsilon$. Experimental results (bars) for $E = 2.3 \times 10^{-5}$, $\omega = 0.07$, and numerical results (squares) for $E = 4 \times 10^{-5}$, $\omega = 0.04$, are compared with the theoretical value of Busse (2010) (dash-dotted line).

and numerical data. Since the function $f(x^2)$ (2.4b) may be considered as constant up to $r \sim 0.6$, which means that the predicted zonal flow is almost a solid-body rotation up to $r \sim 0.6$, we take the average value of the measured $|\bar{U}|/r$ between $r = 0.1$ and $r = 0.6$, i.e. the non-dimensionalized mean angular velocity, and compare it with the theoretical value $0.154\epsilon^2$. Note that experimental results are represented by bars (see for example figure 5) which represent both the uncertainties of the PIV measurements and the deviation of the measured velocity profile from a pure solid-body rotation.

In figure 5 we investigate the influence of the amplitude of libration $\epsilon$ on the zonal flow. Experimentally, we set $E = 2.3 \times 10^{-5}$, $\omega = 0.07$ and systematically change $\epsilon$ between 0.02 and 0.15. To explore a larger range of amplitude we have also performed numerical simulations with $E = 4 \times 10^{-5}$, $\omega = 0.04$ and $\epsilon \in [0.01; 0.2]$. Both experimental and numerical results are quantitatively compatible with the theory with no adjustment parameter. The steady azimuthal velocity scales as $\epsilon^2$ for a large range of $\epsilon$. When $\epsilon$ becomes larger than 0.2, the weakly nonlinear hypothesis cannot be used anymore because terms of higher order cannot be neglected. We also notice that even in a range of values where the condition $\omega \ll \epsilon$ in (2.3) is not fully satisfied, the zonal wind intensity still scales as $\epsilon^2$. In fact, rather than the more restrictive condition (2.3), we only require that (i) $E \ll 1$ to decouple the bulk and boundary layer flows, (ii) $\sqrt{E} \ll \omega \ll 1$ in order to neglect the excitation of inertial waves (Aldridge & Toomre 1969) and to ensure that the spin-up effect of the libration is confined inside the outer boundary layer, and (iii) $\epsilon \ll 1$ to remain in the weakly nonlinear regime.

In figure 6 we report systematic study of the influence of the Ekman number on the zonal flow. Experimental results are compatible with the no-Ekman dependence predicted by Busse (2010) in a large range of Ekman numbers with no adjustment parameter. This is confirmed numerically up to $E \sim 10^{-3}$. For larger values of the Ekman number, the condition (2.3) is not fulfilled and we cannot assume that the effect of spin-up is negligible in the bulk. We have also noticed numerically that further decreasing $E$ for a given $\omega = 0.1$ (which is not so small) leads to a deviation from the theory. Indeed, forced inertial modes are not expected to be negligible anymore and can perturb the zonal flow. In particular, nonlinear self-interaction of these forced modes can drive localized zonal winds (e.g. Morize *et al.* 2010). This
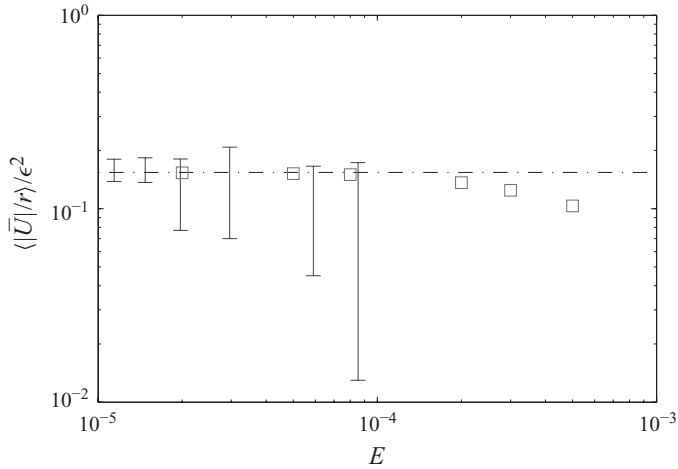
FIGURE 6. Dimensionless average amplitude of $|\bar{U}|/r\epsilon^2$ between $r = 0.1$ and $r = 0.6$ as a function of the Ekman number. Bars are experimental results for $\epsilon = 0.08$ and $\omega = 0.1$ and squares are numerical results for $\epsilon = 0.2$ and $\omega = 0.06$. The dash-dotted line shows the theoretical result of Busse (2010). The velocity profiles have been rescaled by $\epsilon^2$ following the results presented in figure 5. Experimentally, error bars increase with the Ekman number mainly because our experimental set-up does not allow us to average the velocity on a sufficient number of periods when increasing $E$.
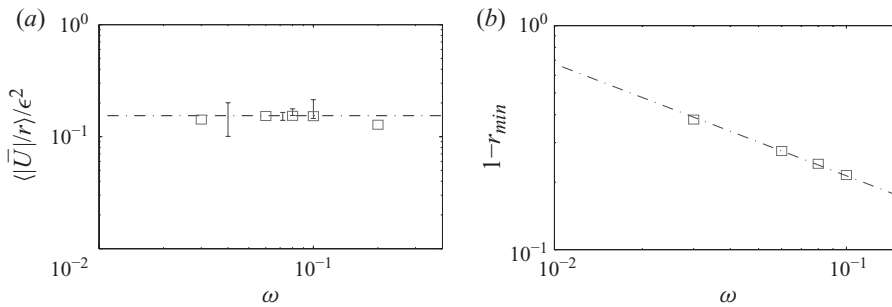


FIGURE 7. (a) Dimensionless average amplitude of $|\bar{U}|/r\epsilon^2$ between $r = 0.1$ and $r = 0.6$ as a function of the frequency of libration $\omega$; squares are numerical values ($E = 5 \times 10^{-5}$, $\epsilon = 0.2$) and bars are experimental data ($E = 1.5 \times 10^{-5}$, $\epsilon = 0.1$). The dash-dotted line shows the theoretical result of Busse (2010). The velocity profiles have been rescaled by $\epsilon^2$ following the results presented in figure 5. (b) Distance of the minimum of the velocity profile from the outer boundary as a function of $\omega$ obtained by numerical simulation for $E = 5 \times 10^{-5}$, $\epsilon = 0.2$. The dotted line scales as $1/\sqrt{\omega}$, which is representative of a skin effect.

peculiar behaviour appears outside the asymptotic limit (2.3) under consideration here and will be the subject of a future study.

Figure 7(a) shows that the amplitude of the zonal wind in the bulk does not depend on $\omega$, as suggested by Busse (2010). Nevertheless, as seen in figure 4, the flow near the outer wall changes with $\omega$. We expect this prograde flow to be related to the same mechanism of boundary layer ejection near the critical latitude as the prograde jets described by Noir *et al.* (2009). To quantify the distance at which the real flow deviates from the analytical solution, we identify the value $r_{min}$ where the velocity has a minimum. The thickness of the layer where the prograde flow develops is shown in figure 7(b) and is found to scale as $1/\sqrt{\omega}$, which is representative of a skin effect.

Therefore, if $\omega$ becomes too small at a fixed $E$, the layer where the effects of external walls are important is visible in the bulk and perturbs the zonal flow.

## 5. Conclusion

In this paper, combining numerical and experimental studies, we report the first quantitative measurements of the steady flow driven by longitudinal librations in a rotating sphere. This approach confirms the main features of the weakly nonlinear theory of Busse (2010): a retrograde differential rotation induced by the libration of the sphere takes place, which may be assimilated to a solid-body rotation for $r < 0.6$. It is also shown that the amplitude of this steady zonal flow is independent of $\omega$ and $E$ and scales as $\epsilon^2$. Note that the same features have been observed experimentally in a librating cylinder (Noir *et al.* 2010) and numerically in a librating spherical shell (Calkins *et al.* 2010) and thus appear to be generic of librating flows.

The main differences between our results and the theoretical profile of Busse (2010) arise close to the outer boundary at the equator. There we observe a prograde flow in a layer of thickness proportional to $1/\sqrt{\omega}$. The analytical resolution of this peculiar feature would necessitate a special treatment since it appears at the critical latitude of the outer boundary layer (Busse 2010). This as well as the experimental study of a librating spherical shell will be the subject of forthcoming studies.

REFERENCES

ALDRIDGE, K. D. & TOOMRE, A. 1969 Axisymmetric inertial oscillations of a fluid in a rotating spherical container. *J. Fluid Mech.* **37**, 307–323.

BUSSE, F. H. 1968 Steady fluid flow in a precessing spheroidal shell. *J. Fluid Mech.* **33**, 739–751.

BUSSE, F. H. 2010 Mean zonal flows generated by librations of a rotating spherical cavity. *J. Fluid Mech.* **650**, 505–512.

CALKINS, M. A., NOIR, J., ELDREDGE, J. & AURNOU, J. M. 2010 Axisymmetric simulations of libration-driven fluid dynamics in a spherical shell geometry. *Phys. Fluids* (in press).

HINDMARSH, A. C., BROWN, P. N., GRANT, K. E., LEE, S. L., SERBAN, R., SHUMAKER, D. E. & WOODWARD, C. S. 2005 Sundials: suite of nonlinear and differential/algebraic equation solvers. *ACM T. Math. Softw.* **31**, 363–396.

MARGOT, J. L., PEALE, S. J., JURGENS, R. F., SLADE, M. A. & HOLIN, I. V. 2007 Large amplitude libration of Mercury reveals a molten core. *Science* **316** (5825), 710–714.

MEUNIER, P. & LEWEKE, T. 2003 Analysis and minimization of errors due to high gradients in particle image velocimetry. *Exp. Fluids* **35** (5), 408–421.

MORIZE, C., LE BARS, M., LE GAL, P. & TILGNER, A. 2010 Experimental determination of zonal winds driven by tides. *Phys. Rev. Lett.* **104**, 214501.

NOIR, J., CALKINS, M. A., LASBLEIS, M., CANTWELL, J. & AURNOU, J. M. 2010 Experimental study of libration-driven zonal flows in a straight cylinder. *Phys. Earth Planet. Inter.* **182**, 98–106.

NOIR, J., HEMMERLIN, F., WICHT, J., BACA, S. M. & AURNOU, J. M. 2009 An experimental and numerical study of librationally driven flow in planetary cores and subsurface oceans. *Phys. Earth Planet. Inter.* **173**, 141–152.

RIEUTORD, M. 1991 Linear theory of rotating fluids using spherical harmonics. II. Time-periodic flows. *Geophys. Astrophys. Fluid Dyn.* **59**, 185–208.

SUESS, S. T. 1971 Viscous flow in a deformable rotating container. *J. Fluid Mech.* **45**, 189–201.

TILGNER, A. 1999 Driven inertial oscillations in spherical shells. *Phys. Rev.* E **59** (2), 1789–1794.

VAN HOOLST, T. V., RAMBAUX, N., KARATEKIN, O., DEHANT, V. & RIVOLDINI, A. 2008 The librations, shape and icy shell of Europa. *Icarus* **195** (1), 386–399.